



# OPEN Modulation of HER2 internalization enhances single-dose antibody-drug potency in HER2<sup>+</sup> gastric cancer

Abbey Zidel<sup>1,6</sup>, Alex Benton<sup>1,2,6</sup>, Emma Brown<sup>1</sup>, Shayla Shmuel<sup>1</sup>, Alex Vanover<sup>1</sup>, Sandeep Surendra Panikar<sup>1</sup>, Ron Bose<sup>3</sup>, Haeseong Park<sup>4</sup>, Andrew A. Davis<sup>5</sup> & Patrícia M. R. Pereira<sup>1</sup>✉

HER2 is a membrane receptor tyrosine kinase overexpressed in 18–20% of gastric tumors. Trastuzumab emtansine (T-DM1) is an antibody-drug conjugate (ADC) that targets HER2-positive (HER2<sup>+</sup>) cancer cells with a chemotherapeutic agent, emtansine. T-DM1 has low efficacy in HER2<sup>+</sup> gastric cancer. This study explored the efficacy of combining drugs known to modulate HER2 internalization to enhance T-DM1 efficacy in gastric cancer. We used cholesterol-depleting drugs (lovastatin) to enhance HER2 membrane density. The irreversible pan-HER tyrosine kinase inhibitor neratinib was used to enhance the internalization of HER2-bound T-DM1. Therapy, pre-treatment and post-treatment positron emission tomography/computed tomography (PET/CT) were performed in both male and female mice. An enhancement of cell surface and internalized HER2 was observed after lovastatin and neratinib incubations, respectively. The combination of lovastatin with neratinib enhanced T-DM1 internalization in cancer cells. A decrease in HER2 protein levels and HER2 phosphorylation was detected in cells treated with T-DM1/lovastatin/neratinib when compared to control and T-DM1-only groups. PET/CT imaging of mice in the T-DM1/lovastatin/neratinib group showed a decrease in HER2 tumoral expression, which was associated with a decrease in tumor volume and sustained treatment efficacy in the T-DM1/lovastatin/neratinib group. This work demonstrates the therapeutic enhancement of T-DM1 using combination therapy with lovastatin/neratinib in gastric cancer. The treatment can be successfully monitored through PET/CT imaging.

**Keywords** HER2, T-DM1, Neratinib, Statin, ImmunoPET

Human epidermal growth factor receptor 2, HER2, is a membrane receptor overexpressed in about 17.9% of gastric cancers<sup>1–4</sup>. Gastric tumors are characterized by a heterogeneous pattern of HER2 expression, which can hinder response to HER2-targeted therapy<sup>5</sup>. Beyond the observed efficacy for the HER2-targeting antibody trastuzumab and the antibody-drug conjugate (ADC) trastuzumab deruxtecan (reviewed recently in<sup>3</sup>), clinical trials failed to demonstrate efficacy for other HER2-targeting antibodies.

Trastuzumab emtansine (T-DM1) is a HER2-directed antibody (trastuzumab) conjugated with the emtansine (DM1) payload<sup>6,7</sup>. Emtansine is cytotoxic to HER2<sup>+</sup> cells by inducing cell arrest and apoptosis through disruption of microtubule function<sup>6</sup>. T-DM1 is used in the clinic for both adjuvant treatment of patients with HER2<sup>+</sup> breast cancer with residual disease at surgery and those with HER2<sup>+</sup> metastatic breast cancer<sup>8,9</sup>. However, patients with HER2<sup>+</sup> gastric cancer have demonstrated poor response to T-DM1 treatment<sup>6</sup>, warranting novel strategies to be explored in preclinical models. The GATSBY clinical trial demonstrated that T-DM1 was not superior to taxane treatment in HER2<sup>+</sup> gastric cancer patients, with median T-DM1 overall survival of 7.9 months and

<sup>1</sup>Department of Radiology, Mallinckrodt Institute of Radiology, Washington University School of Medicine, St. Louis, MO 63110, USA. <sup>2</sup>Cancer Biology Graduate Program, Washington University School of Medicine, St. Louis, MO, USA. <sup>3</sup>Washington University School of Medicine, 4515 McKinley Avenue, Campus Box 8069, St. Louis, MO, USA. <sup>4</sup>Gastrointestinal Cancer Center, Center for Cancer Therapeutic Innovation, Dana-Farber Cancer Institute, Harvard Medical School, Boston, MA, USA. <sup>5</sup>Division of Oncology, Department of Medicine, Washington University School of Medicine, St. Louis, MO 63110, USA. <sup>6</sup>Abbey Zidel and Alex Benton contributed equally to this work. ✉email: ribeirepereira@wustl.edu

median taxane overall survival of 8.6 months<sup>6</sup>. Additionally, the JACOB and TyTAN clinical trials demonstrated no significant increase in overall survival in patients with HER2<sup>+</sup> gastric cancer utilizing the HER2-targeting antibody pertuzumab or the tyrosine kinase inhibitor lapatinib<sup>10,11</sup>. In contrast with the success of multiple HER2-targeted agents in breast cancer, the failure of these agents in gastric cancer may be explained by spatial and temporal heterogeneity of HER2<sup>+</sup> expression and differences in HER2 staining patterns between breast cancer and gastric cancer<sup>1,12–14</sup>. Further, newer agents, such as trastuzumab deruxtecan that are effective in multiple tumor types including gastric cancer<sup>3</sup>, the magnitude of efficacy is less in gastric cancer than in breast cancer. Such discrepancy observed between HER2<sup>+</sup> breast and gastric cancer highlights the need for exploring novel combination therapies that would enhance therapeutic efficacy in gastric cancer.

Effective binding of T-DM1 to HER2<sup>+</sup> cancer cells, followed by internalization, is required for T-DM1 efficacy<sup>15</sup>. Therefore, this study focused on evaluating drugs known to enhance T-DM1 binding and internalization, lovastatin<sup>16–18</sup> and neratinib<sup>19</sup>, into a combination therapy approach with T-DM1. Lovastatin was included in this work in combination with T-DM1 to enhance the membrane receptor density of HER2, making it more available for T-DM1 binding<sup>16–18</sup>. Lovastatin is a cholesterol-depleting drug that has previously been shown to increase cell-surface HER2 density in gastric cancer cells<sup>16</sup>. Statin use in patients with gastric cancer treated with trastuzumab is associated with enhanced antibody efficacy<sup>17</sup>. Neratinib is an irreversible tyrosine kinase inhibitor that enhances HER2 internalization and degradation<sup>19</sup>. Previous work has demonstrated enhanced ADC internalization and efficacy when combined with neratinib in lung cancer and breast cancer<sup>19–21</sup>. Additionally, clinical trials testing T-DM1 in combination with neratinib in patients with HER2<sup>+</sup> metastatic breast cancer demonstrated the safety and potential clinical efficacy of this drug combination in patients with metastatic HER2<sup>+</sup> breast cancer<sup>22</sup>.

Here, we performed *in vitro* and preclinical studies in HER2<sup>+</sup> gastric tumors using T-DM1 in combination with lovastatin, and neratinib (Fig. 1). *In vitro* studies were also validated in HER2-low breast cancer cells. In addition to therapeutic studies, HER2-targeted positron emission tomography/computed tomography (PET/CT) imaging was used to monitor therapeutic response.

## Materials and methods

### Cell culture

NCIN87 (RRID: CVCL\_1603), a human gastric cancer cell line purchased from the American Type Culture Collection, was grown in Roswell Park Memorial Institute (RPMI)–1640 growth medium. RPMI-1640 cell culture growth medium was supplemented with 2 mM L-glutamine, 10 mM hydroxyethyl piperazineethanesulfonic acid (HEPES), 10% fetal calf serum (FCS), 1 mM sodium pyruvate, 4.5 g/L glucose, and 1.5 g/L sodium bicarbonate.

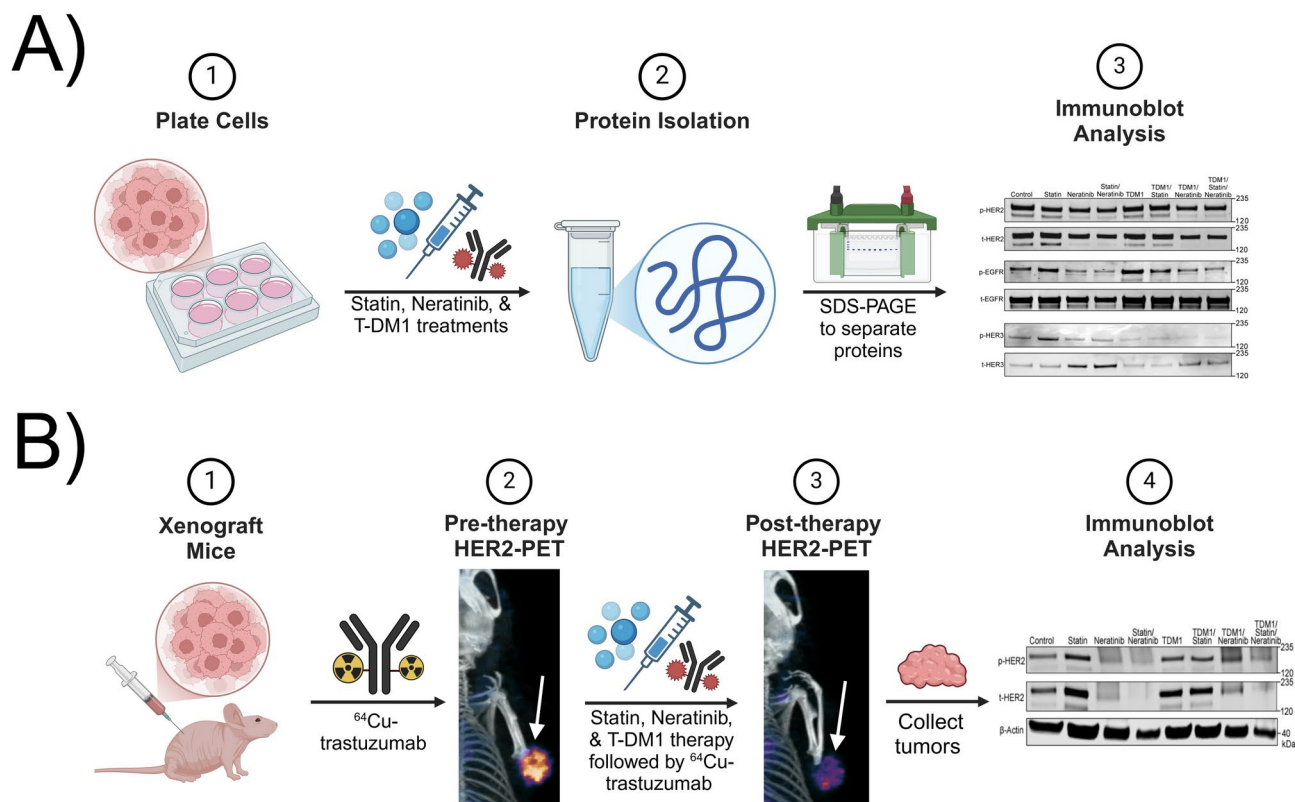


**Fig. 1.** Schematic showing the different *in vitro* and preclinical studies along with the workflow of the procedures used in this work. Scheme made using Biorender.com.

MDAMB361 (RRID: CVCL\_0620), a human breast cancer cell line kindly provided by the Weber Lab, was cultured in DMEM supplemented with 4 mM L-glutamine, 1 mM sodium pyruvate, 4.5 g/L glucose, and 1.5 g/L sodium bicarbonate, and 10% fetal calf serum (FCS).

### Lovastatin, Neratinib, and T-DM1 treatments (*in vitro*)

Cancer cells (2 million) were plated in 6-well plates. Cells were treated at 12 h after plating, and treatment groups included control, lovastatin only, neratinib only, and lovastatin/neratinib combination. Lovastatin was obtained from Thermo Fisher Scientific, and neratinib was purchased from Santa Cruz Biotechnology. Cells in the control group had a media change at 12 h after cell plating and were kept in media throughout the experiment. Cells in the lovastatin treatment groups were treated with fresh culture media containing the active form of the lovastatin drug at a concentration of 25  $\mu$ M for 4 h<sup>16</sup>. Cells in the neratinib treatment groups were treated with 100 nM neratinib for 3 h<sup>19</sup>. Cells in the lovastatin/neratinib combination treatment groups were first treated with lovastatin at 25  $\mu$ M for 4 h<sup>16</sup>. Next, the media was changed, and cells were incubated with neratinib at 100 nM for 3 h<sup>19</sup>. Cells in the T-DM1 incubation groups were treated with 20 nM of T-DM1 for 48 h directly after any previous lovastatin and/or neratinib treatment<sup>17</sup>.

### pHrodo assays

The pHrodo-T-DM1 was obtained by conjugating the free lysine residues of T-DM1 with the amine-reactive pH-sensitive pHrodo iFL Red STP ester dye (ThermoFisher Scientific, P36014) according to the manufacturer's instructions at a molar ratio of 20:1 (dye to T-DM1). Data were collected on an IncuCyte S3 at an interval of 3 h at 37 °C within the Siteman Flow Cytometry Core. The generated quantitative data were exported as Excel files and graphed on GraphPad Prism 9.

### Western blot

Cancer cell lysates or tumor extracts were collected through cell scraping or tissue homogenization. Extracts were centrifuged at 18,000g at 4 °C for 16 min, and supernatants were collected in aliquots for storage at – 80 °C. The Pierce BCA Protein Assay kit (Thermo Fisher Scientific) was used to determine the total protein levels of each sample. Protein (40  $\mu$ g) was loaded in NuPAGE™ 4 to 12% Bis-Tris gels (Invitrogen) and run in 2-(N-morpholino) ethanesulfonic acid (MES) buffer for gel electrophoresis (Invitrogen). After gel electrophoresis, proteins were transferred onto nitrocellulose membranes using the Thermo-Fischer i-Blot gel transfer device (Invitrogen). The membranes were then washed in Tris-buffered saline buffer-tween (TBS-T) before blocking in TBS-T containing either 5% (w/v) nonfat dry milk (Thermo Fisher Scientific) or 5% (w/v) of bovine serum albumin (BSA, Thermo Fisher Scientific). The membranes were incubated with primary antibodies overnight at 4 °C with gentle agitation.

Primary antibodies used in this work included: mouse anti-beta-actin, 1:10,000 (A1978; Sigma, RRID: AB\_476692); rabbit anti-HER2, 1:800 (ab131490; Abcam, RRID: AB\_11157090); rabbit anti-HER2 phospho Y1139, 1:500 (ab53290; Abcam, RRID: AB\_869096); rabbit anti-epidermal growth factor receptor (EGFR), 1:1,000 (ab52894; Abcam, RRID: AB\_869579); rabbit anti-EGFR phospho Y1068, 1:500 (ab40815; Abcam, RRID: AB\_732110); rabbit anti-human epidermal growth factor receptor 3 (HER3), 1:500 (ab32121; Abcam, RRID: AB\_11160022); rabbit anti-HER3 phospho Y1289, 1:2,500 (ab76469; Abcam, RRID: AB\_2293597); mouse anti-extracellular signal-regulated kinase (ERK), 1:100 (14–9108-80; Invitrogen); rabbit anti-pERK, 1:500 (700012; Invitrogen); rabbit anti-protein kinase B (AKT), 1:1000 (9272; Cell Signaling Technology, RRID: AB\_329827); rabbit anti-pAKT, 1:2,000 (4060; Cell Signaling Technology, RRID: AB\_2315049). Primary antibodies were removed the next day, and membranes were washed with TBS-T three times for 10 min each. Secondary antibodies (Invitrogen) were added (either anti-rabbit or anti-mouse, according to the primary antibody used) in a 1:10,000 dilution in the respective blocking buffer. Membranes were incubated with secondary antibodies for 1 h at room temperature. Secondary antibodies were removed, and membranes were washed three times for 10 min each with TBS-T. Membranes were scanned in the Odyssey infrared imaging system (LI-COR Biosciences, RRID: SCR\_014579), followed by FIJI/ImageJ (RRID: SCR\_002285) or Empiria Studio software densitometric band analysis.

Full-length blots are included in the Supplementary Information document.

### Biotin pull down and endocytosis of cell-surface proteins

Cells were plated as described previously in the “Lovastatin, Neratinib, and T-DM1 Treatments (*in vitro*)” section, then washed twice with a solution of cold phosphate-buffered saline (PBS) containing 0.5 mM magnesium chloride (MgCl<sub>2</sub>) and 1 mM calcium chloride (CaCl<sub>2</sub>). Cells were then incubated at 4 °C with gentle rotation with 0.5 mg/mL of EZ-LINK Sulfo-Biotin (Thermo Fisher Scientific) for 30 min, followed by two washes using 100 mM glycine (Thermo Fisher Scientific) in PBS containing 0.5 mM MgCl<sub>2</sub> and 1 mM CaCl<sub>2</sub>.

After cell-surface biotinylation, cell culture medium (pre-warmed) containing 1  $\mu$ M trastuzumab was added to initiate the internalization of cell-surface biotinylated HER2. This step was performed at 37 °C for 90 min, followed by cell incubation on ice for 10 min to stop internalization. Cells were then incubated for 20 min at 4 °C with 50 mM Tris-HCl pH 8.7 (containing 20 mM dithiothreitol (DTT), 100 mM NaCl, 2.5 mM CaCl<sub>2</sub>) to remove unbound cell-surface biotin, followed by rinsing with cold PBS. Cell scraping was performed using radioimmunoprecipitation assay (RIPA) buffer. NeutrAvidin agarose resins (Thermo Fisher Scientific) were used to collect biotinylated cell-surface HER2 using gentle rotation at 4 °C for 2 h with 500  $\mu$ L of RIPA buffer with an equal amount of proteins. NeutrAvidin beads were then washed three times with RIPA buffer and the pooled proteins were resuspended in Laemmli buffer (Thermo Fisher Scientific) before gel electrophoresis.

### Immunofluorescence

NCIN87 cells were plated in 12-well plates on coverslips pre-treated with poly-L-lysine (Sigma). NCIN87 cells were cultured in growth media (500,000 cells per coverslip) and treated with lovastatin, neratinib, both lovastatin and neratinib, or were untreated as described above under “Lovastatin, Neratinib, and T-DM1 Treatments (*in vitro*).” Cells were washed with PBS, followed by fixation in a 4% (v/v) paraformaldehyde solution for 10 min, permeabilization with triton X-100 in PBS (pH 7.4), and blocking in 10% (v/v) goat serum (Millipore) for 30 min. Next, the primary rabbit anti-HER2 antibody (1:100, ab131490, Abcam, RRID: AB\_11157090) was added, followed by a PBS buffer rinse. Cells were then incubated with a secondary fluorescent anti-rabbit antibody (1:200, SC-516248; Santa Cruz Biotechnology). Lastly, cells were washed and images were acquired using the EVOS M5000 Imaging System (Invitrogen, RRID: SCR\_023650) with a 60X oil immersion objective.

### Ethics declarations

All animal experiments were conducted following guidelines approved by Washington University School of Medicine's Research Animal Resource Center and Institutional Animal Care and Use Committee. Experiments were performed under the approved animal protocol ID 24-0274, PI Patricia Ribeiro Pereira. We adhere to the animal research: reporting of *in vivo* experiments (ARRIVE) guidelines and to the guidelines for the welfare and use of animals in cancer research.

### Mouse xenografts

*Nu/nu* male and female mice (6–8 weeks old, Charles River Laboratories, RRID: SCR\_003792) were subcutaneously injected with 5 million NCIN87 cells on the right shoulder (75  $\mu$ L cell suspension mixed with 75  $\mu$ L of reconstituted basement membrane Matrigel, BD Biosciences). The mice were housed in type II polycarbonate cages under the following conditions:  $\sim$ 19–23  $^{\circ}$ C, 30–70% relative humidity, 12 h light/12 h dark cycle. Mice were fed a standard laboratory diet (sterilized), which included sterile water.

Mice euthanasia was performed by controlled carbon dioxide overdose followed by cervical dislocation. Mice anesthesia was performed through inhalation of an oxygen gas mixture containing 1.5–2% isoflurane (Baxter Healthcare).

### *In vivo* therapeutic studies

The male and female *nu/nu* mice began treatment when tumor volumes reached about 215 mm<sup>3</sup> (on average), and mice were randomized into cohorts of 10 mice ( $n = 5$  females and  $n = 5$  males per cohort) each. Tumor dimensions were measured manually twice a week with vernier calipers, and tumor volumes were determined using the following equation (which assumes a spheroid tumor shape), where  $a$  represents the larger caliper measurement and  $b$  represents the shorter caliper measurement:  $V = (4\pi/3) \times (a/2)^2 \times (b/2)$ . Mouse body weights were collected twice a week.

Preclinical treatment groups included the following: saline, lovastatin only, neratinib only, lovastatin/neratinib combination, T-DM1 only, T-DM1/lovastatin combination, T-DM1/neratinib combination, and T-DM1/lovastatin/neratinib combination. Neratinib was prepared in a solution of water containing 0.5% (v/v) methylcellulose. Mice in the saline control group received 200  $\mu$ L saline through oral gavage on days 1 and 2. Mice in the lovastatin or lovastatin combination treatment groups received a dose of 4.15 mg/kg lovastatin through oral gavage with two doses given 12 h apart on days 1 and 2 of treatment<sup>17</sup>. Mice in the neratinib or neratinib combination treatment groups received 20 mg/kg neratinib daily through oral gavage on days 2–6<sup>19</sup>. Mice in the T-DM1 or T-DM1 combination treatment groups received a single dose of 5 mg/kg T-DM1 through intravenous injection on day 2<sup>17</sup>. Mice were daily observed for signs of toxicity, weight loss, or stress. Mice were sacrificed following the treatment period or if tumor volumes reached the limit of 1,500 mm<sup>3</sup>. Tumors were collected and flash-frozen for Western blot analyses.

### Positron emission tomography of trastuzumab radiolabeled with Copper-64

Copper-64 (<sup>64</sup>Cu), obtained from the cyclotron facility at Washington University, was used to radiolabel trastuzumab. Trastuzumab was first conjugated with 2-S-(4-Isothiocyanatobenzyl)-1,4,7-triazacyclononane-1,4,7-triacetic acid (trastuzumab-NOTA) (*p*-SCN-Bn-NOTA, Macrocyclics) in a 20-fold molar excess. Trastuzumab solution was buffer-exchanged using 0.1 M 4-(2-hydroxyethyl)-1-piperazineethanesulfonic acid buffer (HEPES, pH 8.5) and the antibody conjugation with NOTA was performed at 4  $^{\circ}$ C overnight under slow agitation conditions<sup>18</sup>.

Following overnight incubation, the trastuzumab-NOTA conjugate was purified using PD-10 desalting columns (Cytiva 17085101), and the solution was concentrated in 0.1 M ammonium acetate buffer at pH 6 using amicon filters with a molecular cutoff of 50 kDa. Radiolabeling was performed during 1 h incubation at 37  $^{\circ}$ C in 0.1 M ammonium acetate buffer (pH 6). The radiochemical yield and purity were quantified using a mobile phase of a 1:1 mixture of 0.1 M ammonium acetate buffer (pH 6) with 50 mM ethylenediaminetetraacetic acid (EDTA). For stability under different conditions, the radiolabeled antibody was incubated at 4  $^{\circ}$ C in PBS (Gibco) or at 37  $^{\circ}$ C in RPMI-1640 media (Sigma) supplemented with 10% fetal bovine serum and a mixture of penicillin/streptomycin (Sigma). The radiochemical purity of the fractions was then assessed by radio-iTLC. Radiochemical yields ranged from 87 to 99%, and radiochemical purity was 99%, with molar activities ranging from 47.4 to 69.6 MBq/nmol. After radiolabeling, [<sup>64</sup>Cu]Cu-NOTA-trastuzumab was purified and concentrated using PD-10 desalting columns and 50 kDa Amicon filters as described above.

Mice in each treatment group were administered with [<sup>64</sup>Cu]Cu-NOTA-trastuzumab through intravenous injection pre-therapy and post-therapy. At 24 h after [<sup>64</sup>Cu]Cu-NOTA-trastuzumab injection, mice were anesthetized through inhalation of an oxygen gas mixture containing 1.5–2% isoflurane (Baxter Healthcare). The mice were then imaged using the Mediso nanoScan PET/CT scanner (Mediso) at the preclinical imaging



facility of Washington University in St. Louis. The images were analyzed using 3D Slicer software (version 5.0.3; <https://www.slicer.org/>, RRID: SCR\_005619) or Imalytics Preclinical software (version 3.1, Gremse-IT<sup>23</sup>, <http://exmi.rwth-aachen.de/>). PET images were calibrated as a percentage of injected dose per mL (%ID/mL) and scaled from 0 (min) to 35 (max). Regions of interest (ROI) were delineated in the tumor, and activity values were obtained as %ID/mL. The values represented in the graph were expressed as mean uptake %ID/mL in the tumor.

### Statistical analyses

Analyses were conducted using GraphPad Prism version 10.00 ([www.graphpad.com](http://www.graphpad.com), RRID: SCR\_002798). Statistical comparisons of mean values between experimental groups were carried out using analysis of variance (ANOVA) followed by Student's *t*-tests. *P*-values lower than 0.05 were considered statistically significant.

## Results

### Lovastatin plus neratinib enhance HER2 and T-DM1 internalization

This study (Fig. 1) aimed to utilize lovastatin<sup>16–18</sup> and neratinib<sup>19</sup> combination treatment to temporally upregulate cell-surface HER2 density (allowing T-DM1 to effectively bind) and enhance T-DM1—bound HER2 internalization, respectively. Figure 2A illustrates the objectives of this study. First, lovastatin temporally and reversibly upregulated membrane HER2 levels<sup>16,17</sup>, resulting in high levels of available HER2 on the cell surface for T-DM1 to bind. After T-DM1 binding, neratinib was added to enhance HER2 internalization<sup>19</sup>, resulting in an enhancement in HER2-bound T-DM1 internalization.

To visualize the effects of lovastatin and neratinib on HER2 localization, an immunofluorescence assay was performed using the HER2<sup>+</sup> gastric cancer NCIN87 cell line, as shown in Fig. 2B. Similar to our previous observations<sup>16</sup>, we detected an increase in membrane HER2 density in the lovastatin condition as compared to the control. An increase in HER2 and T-DM1 (using pH-sensitive dye pHrodo-T-DM1, Fig. 2C and Supplementary Fig. 1) internalization was observed in both the neratinib and lovastatin/neratinib conditions as compared to the control.

We then assessed HER2 internalization through Western blot using a biotinylation assay to collect internalized HER2. As demonstrated in Fig. 2D and Supplementary Fig. 2, lovastatin/neratinib increased HER2 internalization when compared with control, lovastatin, or neratinib alone.

Overall, these data suggest that the lovastatin/neratinib treatment combination enhanced HER2 and T-DM1 internalization when compared with control, lovastatin, or neratinib treatment conditions.

### T-DM1/Lovastatin/Neratinib decreases HER signaling

Data shown in Fig. 2 suggested an enhancement in HER2-bound trastuzumab internalization using lovastatin/neratinib combination treatment, leading us to investigate the effects of the treatment combinations on proteins involved in HER signaling. Treatment groups of NCIN87 cells included control, lovastatin, neratinib, lovastatin/neratinib, T-DM1, T-DM1/lovastatin, T-DM1/neratinib, and T-DM1/lovastatin/neratinib.

HER2, EGFR, and HER3 protein levels, as well as proteins downstream in the HER signaling pathway, including ERK and Akt, were analyzed by Western blot (Fig. 3 and Supplementary Figs. 3–9).

Higher depletion of both phosphorylated and total HER2 levels was observed in T-DM1/neratinib and T-DM1/lovastatin/neratinib treatment conditions when compared with T-DM1 and T-DM1/lovastatin. Depletion of phosphorylated EGFR and phosphorylated HER3 was higher in the T-DM1/neratinib and T-DM1/lovastatin/neratinib conditions when compared with T-DM1 and T-DM1/lovastatin conditions, with total EGFR and total HER3 levels remaining fairly constant across treatment conditions. Phosphorylated ERK and phosphorylated Akt levels showed similar results to what was observed for phosphorylated HER, with more depletion among T-DM1/neratinib and T-DM1/lovastatin/neratinib conditions than T-DM1 or T-DM1/lovastatin conditions. Total ERK and total Akt levels were consistent across treatment conditions of interest. Similar Western blot results were obtained in the HER2-low breast cancer cell line MDAMB361 (Supplementary Figs. 10–14).

Altogether, these data suggest that T-DM1/neratinib and T-DM1/lovastatin/neratinib treatment deplete phosphorylated proteins both upstream and downstream in the HER signaling pathway effectively, indicating potential synergism of T-DM1 combined with lovastatin and neratinib.

### Lovastatin plus neratinib enhance T-DM1 efficacy in a single dose

Given the promising *in vitro* data indicating the potential of T-DM1/lovastatin/neratinib in depleting HER signaling (Fig. 3), we tested this therapeutic combination in *nu/nu* mice bearing NCIN87 gastric tumors. First, we confirmed that similar to our previous studies<sup>16,17</sup>, lovastatin enhanced trastuzumab uptake in NCIN87 tumors, as observed by PET and quantified by *ex vivo* biodistribution (Supplementary Fig. 15). Lovastatin showed a 1.3-fold increase in trastuzumab tumor uptake when compared with the equivalent pro-drug simvastatin. Therefore, the subsequent therapeutic studies testing T-DM1 combination therapies were performed with lovastatin.

In the clinic, T-DM1 is administered every three weeks over the course of several months with the length of administration depending on the treatment<sup>8,9</sup>. Considering the possible side effects that a multiple-dose schedule of T-DM1 can induce<sup>24</sup>, here we determined the potential of utilizing a single dose of T-DM1 in combination with lovastatin and neratinib in a preclinical model of HER2<sup>+</sup> gastric tumors. We aimed to investigate the potential of the T-DM1/lovastatin/neratinib combinatorial approach in reducing T-DM1 toxicity while increasing its effectiveness. Our previous work showed that lovastatin enhances T-DM1 efficacy in a single dose in the NCIN87 model<sup>18</sup>. However, the NCIN87 tumors showed resistance to the T-DM1/lovastatin treatment at around 50 days after treatment initiation, and tumors were not eliminated<sup>18</sup>.

Figure 4A illustrates the schedule for the various treatment groups. Control groups included mice administered with saline. Additional groups included T-DM1 administered in a single dose or in combination

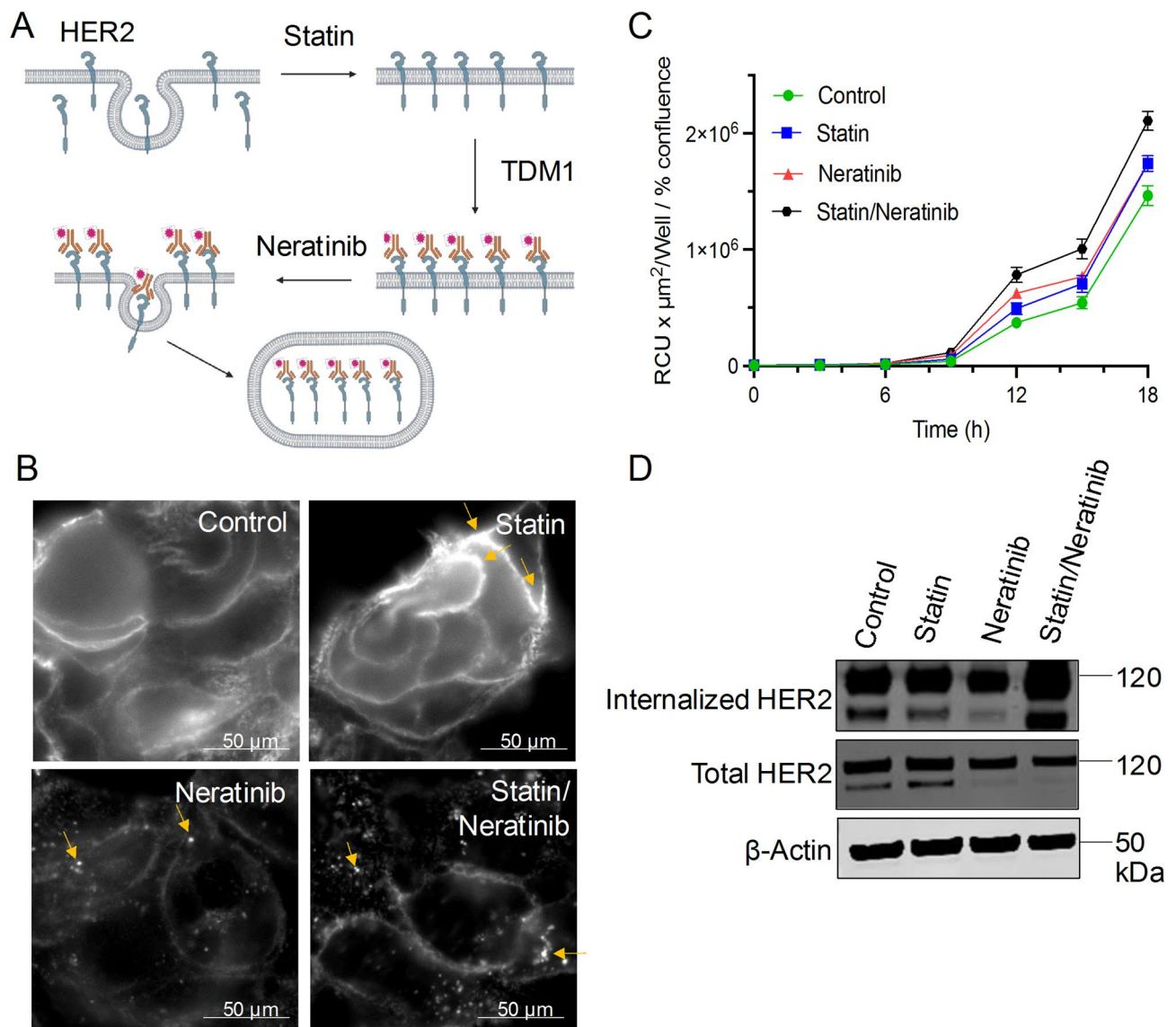


**Fig. 2.** **A** Schematic illustrating expected effects of lovastatin and neratinib on HER2. Lovastatin increases HER2 membrane density<sup>16</sup>, allowing T-DM1 to effectively bind. Neratinib enhances HER2 internalization<sup>19</sup>, thereby enhancing HER2-bound T-DM1 internalization. Schematic created using Biorender.com. **B** Representative immunofluorescence images of control, lovastatin, neratinib, and lovastatin/neratinib conditions. NCIN87 cells were incubated with 25  $\mu\text{M}$  lovastatin for 4 h<sup>16</sup>, with neratinib 100 nM for 3 h<sup>19</sup>, or with a combination of the previously listed concentrations of lovastatin and neratinib. Yellow arrows highlight increased HER2 density at the surface with lovastatin or increased HER2 internalization with neratinib or statin/neratinib. Scale bar = 50  $\mu\text{m}$ . **C** T-DM1 internalization in NCIN87 gastric cancer cells using the pHrodo-T-DM1 dye at 2  $\mu\text{g}/\text{mL}$ . **D** Western blot analyses of internalized HER2 and total HER2 in NCIN87 cells incubated with lovastatin (25  $\mu\text{M}$ , 4 h<sup>16</sup>), neratinib (100 nM, 3 h<sup>19</sup>), or lovastatin/neratinib.  $\beta$ -actin was used as a loading control. Full-length blots are included in the Supplementary Information document.

with lovastatin and neratinib. We used previously reported doses and treatment schedules for lovastatin<sup>16–18</sup> and neratinib<sup>19</sup>. The different therapeutic combinations were tested in both male and female *nu/nu* mice.

No differences in treatment responses were observed between male and female mice, and no changes in mice weight were observed across the treatment groups (Supplementary Fig. 16). Saline and lovastatin-treated mice (control groups) had similar growth trends, with a steady increase in tumor growth and mice were sacrificed at 45 and 50 days after initiating therapy, respectively, due to maximum tumor volume limits reached. Neratinib and lovastatin/neratinib groups showed similar trends to one another, with steady tumor growth at a slower rate than saline and lovastatin groups (Fig. 4B). T-DM1 alone was more effective than the control groups but still showed steady tumor growth. T-DM1/neratinib and T-DM1/lovastatin showed slightly slower tumor growth when compared with T-DM1 alone, but tumor volumes still steadily increased. T-DM1/lovastatin/neratinib

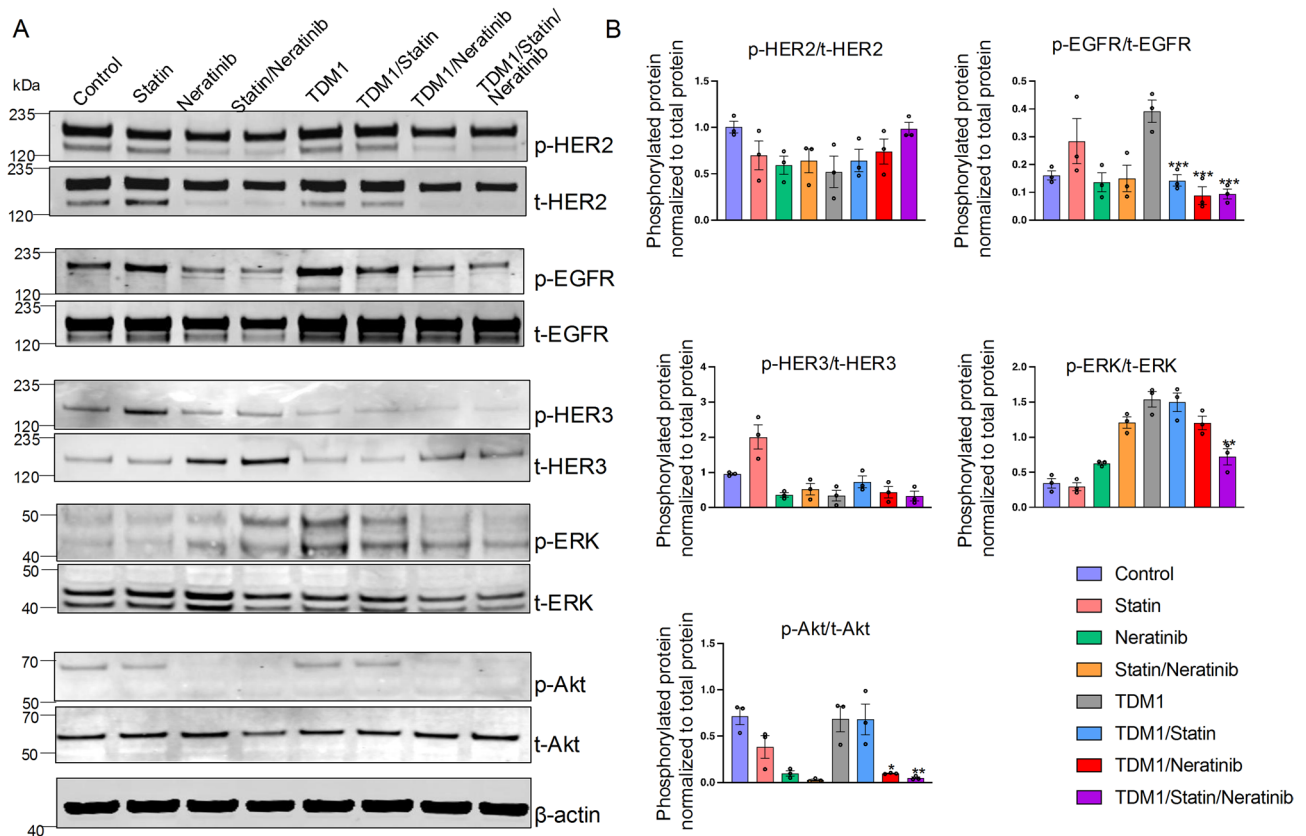


**Fig. 3. A, B** Western blot and quantification of phosphorylated (p) and total (t) levels of HER2, EGFR, HER3, ERK, and Akt in NCIN87 cells.  $\beta$ -actin was used as a loading control. The following conditions were analyzed: control, statin, neratinib, statin/neratinib, T-DM1, T-DM1/lovastatin, T-DM1/neratinib, and T-DM1/lovastatin/neratinib. NCIN87 cells were incubated for 48 h with 20 nM T-DM1 alone or after lovastatin (4 h) and/or neratinib (3 h) treatments<sup>17</sup>. Graph bars (**B**) show quantification of Western blots. Full-length blots are included in the Supplementary Information document. Statistical analyses were performed comparing the treatment groups T-DM1/statin, T-DM1/neratinib, and T-DM1/statin/neratinib to T-DM1 only. Bars,  $n = 3$  per group, mean  $\pm$  S.E.M. \* $P < 0.05$ , \*\* $P < 0.01$ , \*\*\* $P < 0.001$  based on a Student's  $t$  test.

was the most effective treatment combination, and the only treatment schedule able to consistently maintain suppressed tumor growth.

T-DM1/lovastatin/neratinib treatment decreased NCIN87 tumor volume, demonstrating maintained low tumor volume over 60 days when compared to all other treatment groups.

### T-DM1/Lovastatin/Neratinib combination decreases tumoral HER2 protein levels as visualized by PET/CT imaging

The above data show that T-DM1/lovastatin/neratinib decreases HER2 signaling *in vitro* (Fig. 3) and reduces tumor growth *in vivo* (Fig. 4). To monitor HER2 tumor levels in the T-DM1/lovastatin/neratinib therapeutic combination approach, HER2-targeted PET/CT imaging was performed using trastuzumab radiolabeled with copper-64 ( $^{64}\text{Cu}$ -labeled trastuzumab<sup>25</sup>).  $^{64}\text{Cu}$ -labeled trastuzumab was prepared following our previously reported methods<sup>25</sup> (Supplementary Figs. 17, 18).

As shown in Fig. 5A,  $^{64}\text{Cu}$ -labeled trastuzumab was injected on day 1, followed by pre-therapy PET images. On day 29 after therapy initiation,  $^{64}\text{Cu}$ -labeled trastuzumab was administered once again, followed by post-treatment PET imaging on day 30. The mice used in our PET studies had similar tumor volumes when compared with pre- versus post-therapy and they were between 200 and 250 mm<sup>3</sup> so that HER2 levels were monitored by PET imaging before major changes in tumor volume occurred. At day 63 after therapy initiation, tumors were excised and collected for future Western blot analyses.

PET images of T-DM1/neratinib and T-DM1/lovastatin/neratinib groups demonstrated a 1.7–2.4-fold decrease in  $^{64}\text{Cu}$ -labeled trastuzumab uptake from pre- to post-therapy, indicating decreased HER2 expression in these groups (Fig. 5B). No major changes in HER2-PET were observed for the cohorts neratinib or neratinib/lovastatin (Supplementary Fig. 19).

Following tumor excision, Western blot assays were performed with tumor lysates to compare phosphorylated and total HER2 levels across treatment groups (Fig. 5C and Supplementary Figs. 20, 21). T-DM1/lovastatin/neratinib groups demonstrated lower phosphorylated and total HER2 protein levels when compared with T-DM1, T-DM1/neratinib, or T-DM1/lovastatin groups. Altogether, the T-DM1/lovastatin/neratinib combination

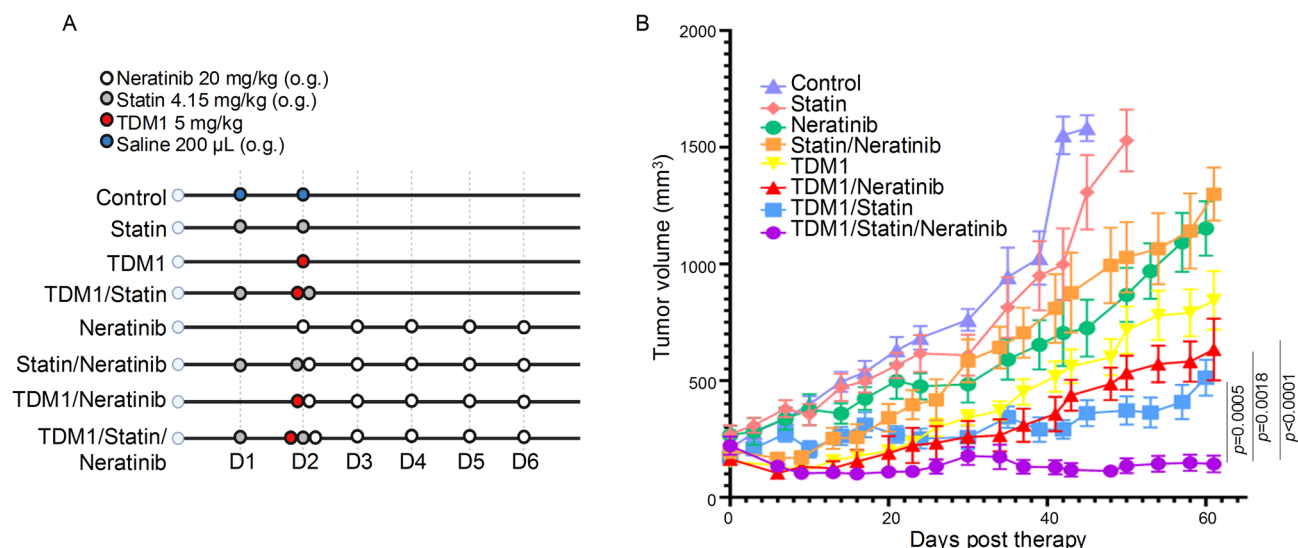


**Fig. 4.** **A** Schematic illustrating treatment schedule. Saline (200  $\mu$ L) was orally administered on days 1 and 2 for the control group. A single intravenous T-DM1 administration (5 mg/kg) was administered on day 2. Lovastatin (4.15 mg/kg) was orally administered 12 h prior to and simultaneously with the intravenous injection of T-DM1 (days 1 and 2). Neratinib (20 mg/kg) was orally administered on days 2–6. Schematic created using Biorender.com. **B** Graph illustrating average tumor volumes ( $\text{mm}^3$ ) for the treatment groups in (A) over the 60-day course of the study, including mean and standard deviation bars. D1–D6, day 1 to day 6.

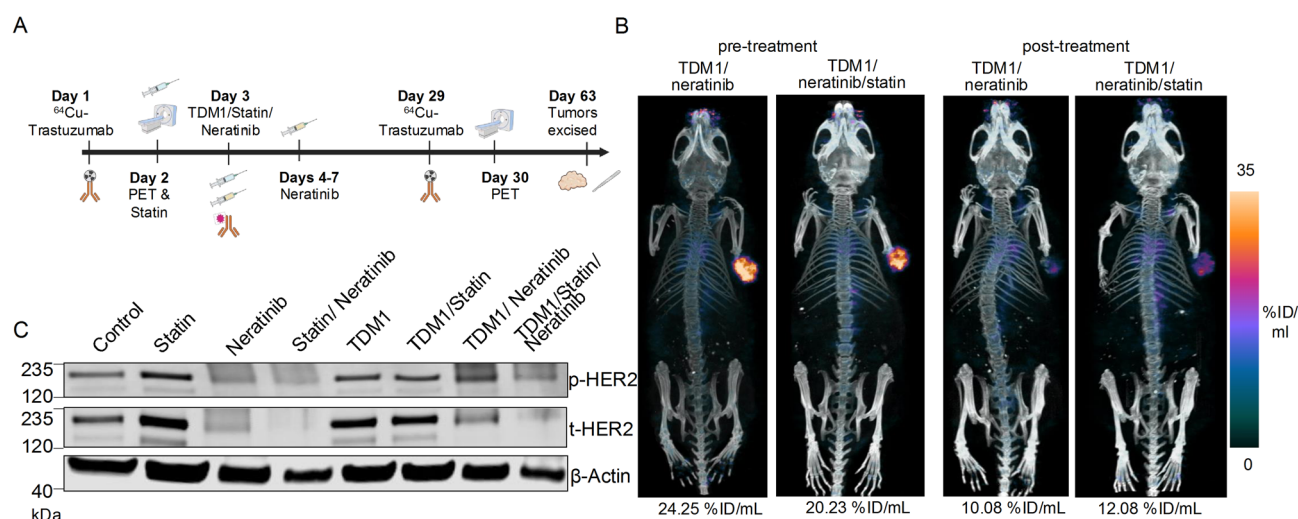


**Fig. 5.** **A** Schematic illustrating  $^{64}\text{Cu}$ -labeled trastuzumab PET/CT before and at 30 days after T-DM1/neratinib or T-DM1/lovastatin/neratinib therapy in *nu/nu* mice bearing NCIN87 tumors. Schematic created using Biorender.com. **B** Representative PET images of  $^{64}\text{Cu}$ -labeled trastuzumab pre-therapy and post-therapy in T-DM1/neratinib or T-DM1/statin/neratinib treatment groups. PET images shown here were calibrated as a percentage of injected dose per mL (%ID/mL) and scaled from 0 (min) to 35 (max). Regions of interest (ROI) were delineated in the tumor, and activity values were obtained as %ID/ $\text{cm}^3$ . The values shown here are expressed as mean uptake %ID/mL in the tumor. **C** Western blot of tumor lysates collected 63 days after therapy showing phosphorylated HER2, total HER2, and  $\beta$ -actin loading control levels in control, statin, neratinib, statin/neratinib, T-DM1, T-DM1/lovastatin, T-DM1/neratinib, T-DM1/lovastatin/neratinib groups. Full-length blots are included in the Supplementary Information document. Scheme made using Biorender.com.



therapy group demonstrated efficacy in treating NCIN87 gastric tumors, and HER2 protein level changes in response to treatment can be monitored using  $^{64}\text{Cu}$ -labeled trastuzumab PET imaging.

## Discussion

While T-DM1 has shown efficacy in treating patients with early-stage and metastatic HER2<sup>+</sup> breast cancer, therapeutic efficacy has not been replicated in preclinical studies<sup>17</sup> or clinical trials<sup>6</sup> for HER2<sup>+</sup> gastric cancer. T-DM1 requires HER2 to be available on the cell surface for effective T-DM1–HER2 binding/internalization and efficacy. Immunofluorescence imaging demonstrated an increase in the staining of membrane HER2 when NCIN87 gastric cancer cells were incubated with lovastatin and an increase in HER2 and T-DM1 internalization when incubated with neratinib (Fig. 2). The observed increase in membrane HER2 and HER2 internalization with the use of lovastatin and neratinib, respectively, is similar to previous reports<sup>16,19</sup>. These observations led us to test a triple combination therapy of T-DM1, along with lovastatin and neratinib, as a novel combination strategy to enhance the efficacy of HER2-targeted therapy in gastric cancer.

Western blot analyses demonstrated a reduction in total HER2 protein, as well as other proteins in the HER pathway, such as EGFR, HER3, ERK, and Akt in HER2<sup>+</sup> gastric cancer cells (Fig. 3) and HER2-low breast cancer cells (Supplementary figs. 10, 11) treated with the triple T-DM1/statin/neratinib combination therapy. There was a greater decrease in expression of proteins involved in HER2 signaling in the triple combination approach in comparison to T-DM1 alone, T-DM1/lovastatin, and T-DM1/neratinib treatments. Preclinical studies showed efficacy in both female and male mice of the T-DM1/lovastatin/neratinib combination therapy (Fig. 4), resulting in the least tumor volume growth out of the eight treatment combination groups. Pre-treatment and post-treatment (28 days after the start of therapy) PET/CT imaging using  $^{64}\text{Cu}$ -labeled trastuzumab confirmed a reduction in HER2 tumoral levels (Fig. 5), demonstrating the ability of  $^{64}\text{Cu}$ -labeled trastuzumab to noninvasively monitor the response of tumors to HER2-targeted treatment.

HER2 homo- or hetero-dimerization results in the activation of downstream pathways, cell proliferation and differentiation, and tumor development<sup>1</sup>. Previous work showed that T-DM1 alone did not affect phosphorylated HER2, HER3, ERK, or Akt levels, but lovastatin in combination with T-DM1 reduced ERK and Akt phosphorylation<sup>17</sup>. This demonstrates the efficacy of lovastatin in reducing phosphorylated ERK and phosphorylated Akt levels when used in combination with T-DM1<sup>17</sup>. Western blot analyses of proteins upstream (EGFR, HER3) and downstream (ERK, Akt) in the HER signaling pathway showed a decrease in phosphorylated protein levels with higher reduction in the T-DM1/lovastatin and T-DM1/neratinib combination when compared to T-DM1 alone. The greatest depletion in phosphorylated EGFR, HER3, ERK, and Akt protein levels occurred with the T-DM1/lovastatin/neratinib treatment combination. Other pathways may be influenced by the lovastatin and neratinib drug administration. Previous work has demonstrated the potential effects of statins on mitochondrial pathways<sup>26</sup>, and neratinib suppresses the function of mutant K-RAS and YAP in pancreatic cancer<sup>27</sup>.

This study investigated a potential drug combination to enhance a previously developed ADC that was not effective in treating patients with HER2<sup>+</sup> gastric cancer. This work demonstrated enhanced T-DM1 efficacy when used as a single dose in combination with lovastatin and neratinib, both *in vitro* and *in vivo*. Our *in vitro* studies showing downregulation of pHER and HER signaling in a HER2-low cancer cell line suggest the potential of testing ADC/statin/neratinib in HER2-low tumor models and future studies are planned in this direction. Currently, T-DM1 is often given in multiple doses in the clinic, leading to negative clinical side effects, most commonly including nausea, fatigue, headache, thrombocytopenia, and constipation<sup>28</sup>. The efficacy of a single dose of T-DM1 in the T-DM1/lovastatin/neratinib treatment requires investigating this triple combination in future studies. We plan to retrospectively investigate the effect of statin in medical records of patients treated with HER2-directed therapy to compare response differences. T-DM1, lovastatin, and neratinib all have known safety profiles<sup>22,29,30</sup>, and future work should investigate the potential toxicity of these drugs in combination and the effects of these drugs on other cell pathways and/or mechanisms. Utilizing lovastatin has the potential to enhance anti-tumor activity with less toxicity compared to combination chemotherapy approaches.

These preclinical findings showing that lovastatin and neratinib enhance T-DM1 efficacy in HER2<sup>+</sup> gastric tumors also open the door for future work to investigate the use of combination therapies of lovastatin and neratinib in HER2-low tumors or with other HER2-specific ADCs. One HER2-specific ADC of interest is trastuzumab deruxtecan, which was clinically approved to treat HER2<sup>+</sup> gastric cancer in 2021 and has been shown in a preclinical study to inhibit gastric tumor growth when administered in combination with lovastatin<sup>18</sup>. Additionally, future work could study multiple versus single doses of lovastatin and neratinib in combination with ADC and/or to determine the most effective treatment combination with a single dose of the ADC. PET/CT imaging can also be used in future preclinical studies to titrate mice with lovastatin and neratinib, and define doses needed for maximal enhancement of tumoral T-DM1 uptake. Additional work should investigate the combination of lovastatin, neratinib, and T-DM1 in HER2-low tumor models.

The results of this study are very promising, particularly because drugs of known safety profiles were used<sup>22,29,30</sup>, but lack an analysis of the impact of the various treatments on non-tumor organs in the mice. Since T-DM1 does not react with mouse HER2<sup>31</sup>, the preclinical model used in this work does not enable measuring T-DM1 accumulation in these non-tumor organs (the NCIN87 tumors express human HER2). So, future work could investigate these effects through clinical trials. Finally, the temporal modulation of proteins in the HER signaling pathway should be investigated further to determine drug administration time points with maximal efficacy.

Overall, this study investigated the triple combination therapy of T-DM1/lovastatin/neratinib to target HER2<sup>+</sup> gastric cancer, utilizing the HER2 modulation effects of lovastatin and neratinib to enhance the therapeutic efficacy of T-DM1 in a single dose and reduce HER2<sup>+</sup> gastric cancer resistance to this therapy. Additionally, this study utilized  $^{64}\text{Cu}$ -labeled trastuzumab to monitor tumoral HER2 in mice through PET/CT imaging.

These data warrant testing in an interventional clinical trial to evaluate the potential safety and efficacy of this novel approach to enhance the efficacy and delivery of T-DM1 in patients with HER2<sup>+</sup> advanced gastric cancer. Furthermore, this approach could be explored in the future with ADCs and in tumors with low HER2 protein levels beyond HER2<sup>+</sup> gastric cancer. Future studies could also focus on titrating mice with neratinib or lovastatin and utilizing HER2-PET to optimize the dose of neratinib and lovastatin *in vivo* that result in an improvement in ADC accumulation in tumors, potentially leading to even more effective treatment strategies.

## Conclusion

This study demonstrated that T-DM1, administered in combination with lovastatin and neratinib, enhanced therapeutic efficacy in gastric tumor xenografts in a single dose both *in vitro* and *in vivo*. Additionally, <sup>64</sup>Cu-labeled trastuzumab PET/CT imaging was able to monitor the response of mice to HER2-targeted therapy through pre-treatment and post-treatment noninvasive imaging. T-DM1, lovastatin, and neratinib in combination showed effective suppression of HER2<sup>+</sup> gastric tumor growth when compared to the other treatment combinations, demonstrating the potential for this drug combination therapy to be used in future clinical trials to enhance ADC efficacy in patients.

## Data availability

Data is provided within the manuscript or supplementary information files.

Received: 19 January 2025; Accepted: 9 May 2025

Published online: 15 May 2025

## References

- Ma, C. et al. Challenges and future of HER2-positive gastric cancer therapy. *Front. Oncol.* **13**, 1080990 (2023).
- Van Cutsem, E. et al. HER2 screening data from ToGA: targeting HER2 in gastric and gastroesophageal junction cancer. *Gastric Cancer*. **18** (3), 476–484 (2015).
- Yoon, J. & Oh, D. Y. HER2-targeted therapies beyond breast cancer—an update. *Nat. Rev. Clin. Oncol.* **21**, 675–700 (2024).
- Oh, D. Y. & Bang, Y. J. HER2-targeted therapies - a role beyond breast cancer. *Nat. Reviews Clin. Oncol.* **17** (1), 33–48 (2020).
- Rüschhoff, J. et al. HER2 testing in gastric cancer: a practical approach. *Mod. Pathol.* **25** (5), 637–650 (2012).
- Thuss-Patience, P. C. et al. Trastuzumab emtansine versus taxane use for previously treated HER2-positive locally advanced or metastatic gastric or gastro-oesophageal junction adenocarcinoma (GATSBY): an international randomised, open-label, adaptive, phase 2/3 study. *Lancet Oncol.* **18** (5), 640–653 (2017).
- Filis, P. et al. The ever-expanding landscape of antibody-drug conjugates (ADCs) in solid tumors: A systematic review. *Crit. Rev. Oncol. Hematol.* **192**, 104189 (2023).
- von Minckwitz, G. et al. Trastuzumab emtansine for residual invasive HER2-positive breast cancer. *N. Engl. J. Med.* **380** (7), 617–628 (2018).
- Verma, S. et al. Trastuzumab emtansine for HER2-positive advanced breast cancer. *N. Engl. J. Med.* **367** (19), 1783–1791 (2012).
- Satoh, T. et al. Lapatinib plus Paclitaxel versus Paclitaxel alone in the second-line treatment of HER2-amplified advanced gastric cancer in Asian populations: TyTAN—a randomized, phase III study. *J. Clin. Oncol.* **32** (19), 2039–2049 (2014).
- Tabernero, J. et al. Pertuzumab plus trastuzumab and chemotherapy for HER2-positive metastatic gastric or gastro-oesophageal junction cancer (JACOB): final analysis of a double-blind, randomised, placebo-controlled phase 3 study. *Lancet Oncol.* **19** (10), 1372–1384 (2018).
- Kaito, A. et al. HER2 heterogeneity is a poor prognosticator for HER2-positive gastric cancer. *World J. Clin. Cases*. **7** (15), 1964–1977 (2019).
- Bang, K. et al. Association between HER2 heterogeneity and clinical outcomes of HER2-positive gastric cancer patients treated with trastuzumab. *Gastric Cancer*. **25** (4), 794–803 (2022).
- Haffner, I. et al. HER2 expression, test deviations, and their impact on survival in metastatic gastric cancer: results from the prospective multicenter VARIANZ study. *J. Clin. Oncol.* **39** (13), 1468 (2021).
- Drago, J. Z., Modi, S. & Chandarlapaty, S. Unlocking the potential of antibody-drug conjugates for cancer therapy. *Nat. Reviews Clin. Oncol.* **18** (6), 327–344 (2021).
- Pereira, P. M. R. et al. Caveolin-1 mediates cellular distribution of HER2 and affects trastuzumab binding and therapeutic efficacy. *Nat. Commun.* **9** (1), 5137 (2018).
- Pereira, P. M. R. et al. Caveolin-1 Temporal modulation enhances antibody drug efficacy in heterogeneous gastric cancer. *Nat. Commun.* **13** (1), 2526 (2022).
- Brown, E. L. et al. Immuno-PET detects antibody–drug potency on coadministration with Statins. *J. Nucl. Med.* **64** (10), 1638–1646 (2023).
- Li, B. T. et al. HER2-mediated internalization of cytotoxic agents in ERBB2 amplified or mutant lung cancers. *Cancer Discov.* **10** (5), 674–687 (2020).
- Bose, R. et al. Irreversible inhibition of HER2 activating mutations with neratinib enhances the pre-clinical efficacy of trastuzumab emtansine and trastuzumab deruxtecan. Cancer Research, 2021. In: Proceedings of the 2020 San Antonio Breast Cancer Virtual Symposium; Dec 8–11; San Antonio, TX. Philadelphia (PA): AACR; Cancer Res 2021;81(4 Suppl):Abstract nr PS4-13. (2020).
- Li, S. et al. Neratinib Synergizes with Trastuzumab Antibody Drug Conjugate or with Vinorelbine to Treat HER2 Mutated Breast Cancer Patient-Derived Xenografts and Organoids (bioRxiv, 2023).
- Abraham, J. et al. Safety and efficacy of T-DM1 plus neratinib in patients with metastatic HER2-positive breast cancer: NSABP foundation trial FB-10. *J. Clin. Oncol.* **37** (29), 2601–2609 (2019).
- Gremse, F. et al. Imalytics preclinical: interactive analysis of biomedical volume data. *Theranostics* **6** (3), 328–341 (2016).
- Pondé, N. et al. Trastuzumab emtansine (T-DM1)-associated cardiotoxicity: pooled analysis in advanced HER2-positive breast cancer. *Eur. J. Cancer*. **126**, 65–73 (2020).
- Simo, C. et al. [<sup>64</sup>Cu]Cu-NOTA-Trastuzumab and [<sup>89</sup>Zr]Zr-DFO-Trastuzumab in Xenografts with Varied HER2 Expression. *Mol. Pharm.* **21** (12), 6311–6322 (2024).
- Mollazadeh, H. et al. Effects of Statins on mitochondrial pathways. *J. Cachexia Sarcopenia Muscle*. **12** (2), 237–251 (2021).
- Dent, P. et al. Neratinib inhibits Hippo/YAP signaling, reduces mutant K-RAS expression, and kills pancreatic and blood cancer cells. *Oncogene* **38** (30), 5890–5904 (2019).
- Diéras, V. et al. Trastuzumab emtansine in human epidermal growth factor receptor 2–positive metastatic breast cancer: an integrated safety analysis. *J. Clin. Oncol.* **32** (25), 2750–2757 (2014).
- Juarez, D. & Fruman, D. A. Targeting the mevalonate pathway in cancer. *Trends Cancer*. **7** (6), 525–540 (2021).

30. Singh, H. et al. U.S. Food and drug administration approval: neratinib for the extended adjuvant treatment of early-stage HER2-positive breast cancer. *Clin. Cancer Res.* **24** (15), 3486–3491 (2018).
31. Lewis Phillips, G. et al. Trastuzumab does not bind rat or mouse ErbB2/neu: implications for selection of non-clinical safety models for trastuzumab-based therapeutics. *Breast Cancer Res. Treat.* **191** (2), 303–317 (2022).

## Acknowledgements

We thank the Washington University School of Medicine isotope production team for the production of copper-64 and the small animal imaging facility. The Preclinical Imaging Facility was supported by NIH/NCI Siteman Cancer Center (SCC) Support Grant P30 CA091842, NIH instrumentation grants S10OD018515 and S10OD030403, and internal funds provided by the Mallinckrodt Institute of Radiology. We thank the Alvin J. Siteman Cancer Center at Washington University School of Medicine and Barnes-Jewish Hospital in St. Louis, MO., for the use of the Siteman Flow Cytometry, which provided IncuCyte S3 Live Cell Analyzer service. The Siteman Cancer Center is supported in part by an NCI Cancer Center Support Grant #P30 CA091842. We thank Na-Keysha Berry for her assistance with mouse monitoring. We thank Dr. Jason Lewis for the discussions regarding this work.

## Author contributions

A.Z. contributed to the acquisition, visualization/interpretation, and analysis of data (Figs. 1–5), data visualization, and had major contributions of writing—original draft and review & editing. A.B. contributed to the acquisition, visualization/interpretation, and analysis of data related to the studies with the breast cancer cell lines, and pHrodo assays, and had major contributions during manuscript revisions. E.L.B. contributed to the experimental design, acquisition and visualization/interpretation of data presented in Figs. 2B and 2D, 3, 4 and 5, and had major contributions to writing—review & editing. S.S. monitored tumor growth (male mice), assisted with the collection of data for *in vitro* and *in vivo* studies, performed data analyses, and had major contributions to writing—review & editing. A.V. assisted with the collection of data related to the radiolabeling and stability studies. S.S.P. contributed to immunofluorescence studies (Figure 1B) and imaging studies. R.B. Conceptualization, Writing—review & editing. H.P. Conceptualization, Writing—review & editing. A.D. Conceptualization, Writing—review & editing. P.R.P. Conceptualization, Data curation, Formal analysis, Funding acquisition, Investigation, Methodology, Project administration, Resources, Supervision, Validation, Visualization, Writing—original draft, Writing—review & editing.

## Declarations

## Competing interests

AAD participates in Scientific Advisory Boards for Pfizer and Biotheranostics (unrelated to the studies that are described here). The other authors declare no potential conflicts of interest.

## Disclosures

PMRP reports grants from the NIH, Breast Cancer Alliance, the Siteman Cancer Center, and The Elsa Pardee Foundation during the conduct of the study. AAD reports a grant from the Breast Cancer Alliance. No disclosures were reported by the other authors.

## Additional information

**Supplementary Information** The online version contains supplementary material available at <https://doi.org/10.1038/s41598-025-01947-7>.

**Correspondence** and requests for materials should be addressed to P.M.R.P.

**Reprints and permissions information** is available at [www.nature.com/reprints](http://www.nature.com/reprints).

**Publisher's note** Springer Nature remains neutral with regard to jurisdictional claims in published maps and institutional affiliations.

**Open Access** This article is licensed under a Creative Commons Attribution-NonCommercial-NoDerivatives 4.0 International License, which permits any non-commercial use, sharing, distribution and reproduction in any medium or format, as long as you give appropriate credit to the original author(s) and the source, provide a link to the Creative Commons licence, and indicate if you modified the licensed material. You do not have permission under this licence to share adapted material derived from this article or parts of it. The images or other third party material in this article are included in the article's Creative Commons licence, unless indicated otherwise in a credit line to the material. If material is not included in the article's Creative Commons licence and your intended use is not permitted by statutory regulation or exceeds the permitted use, you will need to obtain permission directly from the copyright holder. To view a copy of this licence, visit <http://creativecommons.org/licenses/by-nc-nd/4.0/>.

© The Author(s) 2025